1 **Replicated Functional Evolution in Cichlid Adaptive Radiations**

2

3 Christopher M. Martinez[1,*,**], Katherine A. Corn[2,3,4,**], Sarah Williamson[2], Darien Satterfield[2],

4 Alexus S. Roberts-Hugghis[2], Anthony Barley[4], Samuel R. Borstein[6], Matthew D. McGee[7], and

5 Peter C. Wainwright[2]

6

7 [1]Department of Ecology and Evolutionary Biology, University of California, Irvine, 92697, USA

8 [2]Department of Evolution and Ecology, University of California, Davis, 95616, USA

9 [3]Department of Biological Sciences, Virginia Polytechnic Institute and State University,

10 Blacksburg, VA, 24061, USA

11 [4]School of Biological Sciences, Washington State University, Pullman, WA, 99163, USA

12 [5]School of Mathematical and Natural Sciences, Arizona State University–West Campus,

13 Glendale, AZ, 85306, USA

14 [6]Department of Ecology and Evolutionary Biology, University of Michigan, Ann Arbor, MI,

15 USA

16 [7]School of Biological Sciences, Monash University, Melbourne, Victoria, Australia

17

18 *Correspondence: c.martinez@uci.edu (C.M.M)

19

20 **Authors contributed equally to this paper.

21

ABSTRACT

Adaptive radiations highlight the mechanisms by which species and traits diversify and the extent to which these patterns are predictable. We used 1,110 high-speed videos of suction feeding to study functional and morphological diversification in 300 cichlid species from three African Great Lake radiations of varying ages (Tanganyika, Malawi and Victoria) and an older, spatially dispersed continental radiation in the Neotropics. Among African radiations, standing diversity was reflective of time. Morphological and functional variance in Lake Victoria, the youngest radiation, was a subset of that within Lake Malawi, which itself was nested within the older Tanganyikan radiation. However, functional diversity in Neotropical cichlids was often lower than in Lake Tanganyika, despite being at least 25 My older. These two radiations broadly overlapped, but each diversified into novel trait spaces not found in the youngest lake radiations. Evolutionary rates across radiations were inversely related to age, suggesting, at least for lake radiations, extremely rapid trait evolution at early stages. Despite this support for early bursts, other patterns of trait diversity were inconsistent with expectations of adaptive radiations. This work suggests that cichlid functional evolution has played out in strikingly similar fashion in different radiations, with contingencies eventually resulting in lineage-specific novelties.

Introduction

Adaptive radiations provide glimpses into how traits diversify and evolve across related taxa in the presence of ecological opportunity (Simpson 1953; Gillespie et al. 2020). Studies on adaptive radiations have helped to explain how Caribbean anoles (Losos et al. 1998) and Hawaiian spiders (Gillespie 2004) have colonized new island habitats through repeated evolution of convergent ecomorphs. They have also highlighted mechanisms underlying trait divergence

45 across adaptive peaks in Bahamian pupfishes (Patton et al. 2022), Galapagos finches, and

46 Hawaiian honeycreepers (Tokita et al. 2016). A common theme in the literature on adaptive

47 radiations is the degree to which trait evolution reflects predictable patterns of diversification

48 versus the generation of novel combinations of phenotypes (e.g., Schluter 1996; Losos et al.

49 1998; Gillespie 2013).

50   Cichlid fishes are renowned for having multiple expansive radiations involving hundreds

51 of species in each of three large African lakes – Tanganyika, Malawi and Victoria – (Freyer and

52 Illes 1972) and a continental radiation in tropical South and Central America (López-Fernández

53 et al. 2013; Arbour and López-Fernández 2014). The existence of these large radiations of

54 related species provides an opportunity to capitalize on natural replication to address questions

55 about the repeatability of these systems at a scale beyond the first few niche expansions. The

56 radiations also differ considerably in age, approximately 55 Ma for Neotropical cichlids, 28 Ma

57 for Lake Tanganyika (although a recent estimate suggests 10 Ma; Ronco et al. 2021), 2 Ma for

58 Lake Malawi, and 0.1 Ma for Lake Victoria (we discuss cichlid ages further in the supplement).

59 These differences present temporally spaced sample points that allow insight into the long-term

60 unfolding of adaptive radiations and the relative importance of time and rate of diversification on

61 current patterns of diversity.

62   Previous comparisons of phenotypic diversity in the three African lakes have drawn two

63 main conclusions. First, diversity of body shape and trophic morphology differs between the

64 lakes, with the oldest radiation, in Lake Tanganyika, housing greater diversity of body shape and

65 craniofacial morphology, and the youngest radiation, in Lake Victoria, having the lowest

66 diversity (Young et al. 2009; Cooper et al. 2010). It is not known whether adaptive radiations of

67 the African lakes have amassed greater morphological diversity, and associated functional

68   variation, than the much older continental radiation in the Neotropics that includes roughly 500

69   species (Lopez-Fernandez et al. 2013). Such a contrast would provide insight into whether the

70   processes of adaptive evolution in the African lakes produces even greater diversity than a

71   continental radiation evolving over a much longer time span. Second, convergent ecology and

72   morphology are common, suggesting relatively predictable modes of diversification and broadly

73   repeated patterns of evolution in feeding morphology (Cooper et al. 2010) and body shape

74   (Kocher et al. 1993; Young et al. 2009). Similar instances of convergence have been found in

75   related groups of Neotropical cichlids (Burress et al. 2017). Thus, large cichlid adaptive

76   radiations could generate similar, though not identical, sets of phenotypes where diversity

77   accumulates over extended time periods.

78   The temporal sampling of cichlid radiations creates an opportunity to evaluate, at various

79   stages of development, patterns of functional diversification relative to our expectations of

80   adaptive radiations. A classic prediction is an early burst in trait diversification, where

81   evolutionary rates are initially rapid as open niches in newly colonized habitats are filled,

82   followed by a nonlinear decay in rates after initial expansion (Simpson 1953). An assumption of

83   the early burst model is that the rapid increase in trait diversity is achieved by different lineages

84   evolving toward separate adaptive zones where they subsequently undergo further

85   diversification, resulting in comparatively greater variance among clades than within (Simpson

86   1953; Harmon et al. 2003).

87   In the present study, we describe the diversity of cichlid prey capture kinematics using

88   high-speed video recordings of 300 species, sampled from the three African great lake radiations

89   and the Neotropics. We contrast kinematic and morphological variation of the feeding

90   mechanism in radiations of varying age to test the hypothesis that differences in standing

4

91   functional diversity are due to time, as opposed to different rates of evolution. To assess the

92   repeatability and predictability of cichlid adaptive radiation, we also quantify the extent to which

93   each has produced species with similar feeding kinematics. Additionally, we test the key

94   expectation that adaptive radiations exhibit an early burst in trait diversification that is achieved

95   through the partitioning of traits among clades (Simpson 1953; Harmon et al. 2003).

96   A secondary objective of this work is to examine the relationship between morphological

97   and functional diversity of the cichlid feeding mechanism. Preliminary estimates of body and

98   craniofacial variation in the three large African lake radiations have typically been interpreted as

99   reflecting functional diversity linked to locomotor and feeding biomechanics (Young et al. 2009;

100   Cooper et al. 2010). In many cases, links between morphological variation and functional

101   properties are well-established (Hulsey & García de León 2005; Hulsey et al. 2006; Higham et

102   al. 2007). Nevertheless, our current understanding of functional diversity in cichlids is largely

103   inferred from morphological variation, rather than direct measurements of functional traits.

104   Comparisons of functional diversity allow us to test the reliability of morphological variation to

105   reflect function and help to identify key axes of diversification that are cryptic when only

106   morphology is considered.

107

108   **Methods**

109   ***Species sampling and feeding videos***

110   1,110 high-speed videos of feeding motions from 300 species of lab-filmed cichlids were

111   studied. Species were broadly distributed phylogenetically from one of four focal radiations, the

112   Neotropics (n=85 species) and African Great Lakes, Tanganyika (n=89), Malawi (n=86), and

113   Victoria (n=40). We note that two species, *Harpagochromis sp.* "golden duck" and *Pyxichromis*

114   *orthostoma*, belonging to the Lake Victoria Region Superflock are endemic to Lake Kyoga,

115   which retains a connection to Lake Victoria via the Victoria Nile River. All videos were filmed

116   from a lateral perspective at 2,000 frames-per-second (McGee et al. 2016) and contained full-

117   effort suction feeding strikes on moderately evasive, living midwater prey. Primary prey

118   included mosquito larvae (*Culex pipiens*), black worms (*Lumbriculus* sp.), and *Daphnia magna*.

119   Small fish were rarely used as prey to elicit sufficiently full effort feeding strikes from some

120   species, which was important for reducing kinematic variation due to fish effort. We extracted 10

121   frames from each video, equally spaced in time from the initiation of the motion to peak

122   expansion of the feeding apparatus, prior to mouth closing. For comparative analyses, we

123   matched filmed species to a recent cichlid phylogeny (McGee et al. 2020; Supplementary

124   Information).

125

126   ***Morphological and functional traits***

127   Cichlid functional diversity was determined using a variety of kinematic traits, all derived

128   from an initial configuration of 18 cranial landmarks manually placed on each of 10 video

129   frames for a motion (fig. 1A). Digitizing was done in tpsDIG2 (Rohlf 2015) and StereoMorph

130   (Olsen and Westneat 2015). Landmark data for 53 species came from a previous study (Martinez

131   et al. 2018) but the remaining 247 species comprised new data. First, subsets of landmarks were

132   used to measure movements (i.e., maximum excursions) of key morphological features involved

133   in prey capture. In total, we created six *motion component* traits (fig. 1B), three from rotational

134   movements of bones (*lower jaw rotation*, *cranial rotation*, *maxillary rotation*) and three from

135   linear displacements (*premaxilla protrusion*, *hyoid depression*, *mouth gape*). We analyzed traits

136   both as multivariate *motion components*, and individually. Due to the incommensurability of

6

137 angles and linear displacements (Huttegger and Mitteroecker 2011), we converted the three

138 rotational traits to distances by using the observed angle of rotation and the length of the rotating

139 arm (measured on the fish at full gape) to determine the length of the arc transcribed by the

140 structure in question (e.g., the Euclidean distance travelled by the distal end of the maxilla). All

141 component traits were then scaled by dividing values by the centroid size of the fish's head in a

142 closed-mouth state. Lastly, we averaged the components across repeated feeding trials within

143 individuals, and then across individuals to get a mean trait value for the species. All additional

144 traits described below were similarly averaged to species for comparative analyses.

145　　　　Additional kinematic traits were created using an approach that characterizes movements

146 as trajectories of shape change (fig. 1), integrating the numerous moving parts involved in a

147 complex motion into a single object that allows for comparisons at the whole-motion level

148 (Adams and Cerney 2007; Adams and Collyer 2009; Collyer and Adams 2013; Martinez et al.

149 2018; 2022; Martinez and Wainwright 2019). Digitized cranial landmarks were aligned and

150 scaled using generalized Procrustes analysis (GPA) with the 'gpagen' function in the 'geomorph'

151 package, v 4.0.3, in the R statistical environment, v 4.1.3 (Adams et al. 2021; R Core Team

152 2022), with alignment of sliding semi-landmarks along the ventral margin of the head achieved

153 by minimizing Procrustes distances. Once aligned with GPA, the progressive movements of

154 landmark-tracked cranial features result in a trajectory of shape change (fig. 1A & E), the

155 features of which can be used as traits that capture motion variation (Martinez et al. 2018; 2019;

156 2022). In this study, for example, the length of each motion trajectory is a measure of cranial

157 *kinesis*, or the amount of movement generated by the feeding apparatus during prey capture (fig.

158 1D). The total trajectory length was computed as the sum of Procrustes distances between

159 consecutive motion shapes (Collyer and Adams 2013).

160   We also generated two composite traits designed to provide context about when and how

161   kinesis is achieved. *Kinesis skew* was the natural logarithm of the ratio of kinesis across the final

162   five motion shapes to the total kinesis for the motion. It is a descriptor of the temporal

163   distribution of kinesis within a movement, with smaller values indicating comparatively more

164   movement toward the beginning of the feeding strike and larger values meaning that movement

165   is concentrated near the end of the strike. Next, we measured a *kinesis coefficient* trait, as an

166   analog to kinematic transmission (Westneat 1994; 2004), which is commonly used with

167   biomechanical linkage models to describe output movement of an anatomical feature, given a

168   degree of input motion from another. Here, we took the natural logarithm of total kinesis for a

169   motion (output movement) divided by maximum cranial rotation (input movement) from the

170   *motion components* described above. We used cranial rotation, which is driven by contraction of

171   epaxial muscles posterior to the head, for the input value as it facilitates expansion of the buccal

172   cavity and drive movements of other features of the feeding apparatus (Camp et al. 2020).

173   The final functional trait we compared was *motion pattern*, briefly described here. For

174   complex biomechanical systems composed of numerous mobile features, any change in relative

175   timing and/or degree of movement across those features causes variation in the pattern of

176   movement at the whole-motion level. We used anatomical landmarks to express feeding

177   movements as an ordered series of changing shapes over time, or a trajectory through

178   morphospace (fig. 1A). The paths forged by these trajectories each have their own shape that

179   reflects motion patterns – different trajectory shapes represent different patterns of movement

180   that can be observed both within a single species feeding with different modes of prey capture

181   (Martinez et al. 2022) and across species with different evolved feeding systems (Martinez et al.

182   2018). We note that *Motion components* and *motion pattern* are both multivariate descriptors of

183 feeding movements but capture contrasting aspects of their diversity. *Motion components*

184 measure maximum excursions of key features of feeding motions, whereas *motion pattern*

185 describes how and when those movements take place (Martinez et al. 2022). To compare *motion*

186 *patterns*, we used modified code from the 'trajectory.analysis' function in the R package 'RRPP'

187 (version 1.0.0) to align and scale trajectories (fig. S1; Collyer and Adams 2018; 2019). Here, the

188 centroid size of the entire trajectory was the scaling factor.

189   To provide context to functional and kinematic patterns, we also examined interspecific

190 cranial morphologies across cichlid species. We extracted head shape data from the starting

191 positions of motions, where the mouths were in a closed state. A separate shape alignment was

192 done on head shape landmarks, which were then averaged to species prior to statistical analyses.

193

194 ***Trait diversity and overlap among radiations***

195   Variance of morphological and kinematic traits, both univariate and multivariate, were

196 measured and statistically compared using the 'morphol.disparity' function in 'geomorph' with

197 10,000 permutations. In addition to trait variation, we were interested in the degree of overlap (or

198 lack thereof) in the occupation of multivariate functional and morphological spaces across

199 cichlid radiations. We created four-dimensional hypervolumes for *motion components*, *motion*

200 *pattern*, and head shape data using the R package 'hypervolume' v 3.0.0 (Blonder et al. 2014;

201 2018). We took the first four axes from a principal component analysis, as hypervolumes are best

202 conducted on orthogonal variables (Blonder et al. 2014; 2018). Hypervolumes were made for

203 each radiation (e.g., species from Lake Tanganyika), and for subsets of the data excluding each

204 radiation (e.g., all species *not* from Lake Tanganyika). We then assessed hypervolume overlap

205 and the fraction of unique space occupied by each radiation. Lastly, we estimated the likelihood

206 of our observed results against a null distribution of hypervolumes generated by randomly

207 permuting group assignments among species 10,000 times (e.g., Corn et al. 2022).

208

209 ***Rates of evolution***

210   For all traits, we estimated rates of evolution (the Brownian rate parameter) within each

211 cichlid radiation with the 'compare.evol.rates' function in 'geomorph' for both univariate and

212 multivariate rates, with significance based on 10,000 permutations.

213

214 ***Modes of trait diversification***

215 We examined both historical reconstructions of trait diversification and contemporary patterns of

216 variation to explore the manner by which trait diversity was attained in cichlid radiations. We

217 estimated the accumulation of trait disparity through time (DTT) in radiations using the 'dtt'

218 function in the R package 'geiger' v 2.0.7. (Harmon et al. 2008; Pennell et al. 2014). DTT plots

219 show relative disparities among subclades at each divergence event in the tree, estimating

220 whether trait diversity is concentrated within or among subclades as an explicit test of the early

221 burst expectation (Simpson 1953). An output of this analysis is the morphological disparity index

222 (MDI), a metric for comparing the difference between the estimated relative disparity of a clade

223 and the disparity of the clade under simulated Brownian motion. MDI statistics were calculated

224 for the first 75% of the tree's history, as missing species in the recent phylogeny may obscure

225 patterns close to the present. We estimated DTT from subtrees of each radiation for *motion*

226 *components*, *motion pattern* and head shape, using the first four axes from PCAs on each,

227 consistent with our comparisons of hypervolumes. Tree topology is key to DTT analyses, so we

228 note caution in interpreting results for young radiations, like Lakes Malawi and Victoria, in

229   which a tree-like model of lineage diversification is unlikely due to widespread hybridization

230   (Joyce et al. 2011; Meier et al. 2017; Scherz et al. 2022). Consequently, we focus our discussion

231   on the two older radiations in Lake Tanganyika and the Neotropics but provide results for all

232   radiations in the supplement materials.

233   To further examine patterns of trait dispersion, we computed distances between extant

234   species and radiation-specific ancestral states. For each cichlid radiation, we estimated ancestral

235   states under Brownian motion with the 'gm.prcomp' function in 'geomorph', extracting the value

236   at the root of the tree as the most recent common ancestor (MRCA) for the radiation. Finally, we

237   measured Euclidean distances (*motion components*) and Procrustes distances (*motion pattern* and

238   head shape) between each species and its radiation's MRCA.

239

240   **Results**

241   ***Functional diversity across cichlid radiations***

242   *Motion components*, composed of six key features of fish cranial movement during

243   feeding (fig. 1B), displayed 3.2 (Lake Tanganyika) and 2.9 times (Neotropics) greater variance

244   in older radiations compared to the youngest radiation in Victoria (figs. 2 & 3; table S3).

245   Separate univariate analyses on the individual components did show some variation in rank

246   orders of variances across traits (fig. 2; table S3). In all cases, Lake Victoria had the lowest

247   variance, followed closely by Lake Malawi, but some traits displayed their highest variation in

248   Lake Tanganyika (*premaxillary protrusion*, *maxillary rotation*, *lower jaw rotation*, and *mouth*

249   *gape*), while others were most variable in the Neotropics (*cranial rotation* and *hyoid depression*).

250   Functional traits derived from trajectories of shape change also showed different levels of

251   diversity across radiations. Cranial *kinesis* had significantly greater variance in Lake Tanganyika

11

252 than all other cichlid radiations, having 1.9-times greater variance than the next closest (the

253 Neotropics) and 2.9-times greater variance than the lowest (Lake Victoria). *Kinesis skew*, the

254 proportion of kinesis in the latter half of the feeding motion, was again most variable in Lake

255 Tanganyika, but there was greater parity between it, Lake Malawi and the Neotropics (fig. 2).

256 *Kinematic coefficient*, output kinesis relative to input movement from cranial rotation, showed

257 the highest variance in the Neotropical radiation, which was significantly greater than that of the

258 younger radiations in Lakes Malawi and Victoria (fig. 2). Finally, the rank order of variances for

259 whole *motion pattern*, a trait describing the timing and sequence of motion events, was the same

260 as they were for *kinesis skew* – Lake Victoria was significantly lower than the other major

261 radiations, followed by nearly identical values in Lake Malawi and the Neotropics, and the

262 greatest variance again in Lake Tanganyika (fig. 2 & 3). Despite its young age, Lake Malawi

263 showed surprisingly high diversity in *motion pattern*. This appears to be driven by a collection of

264 species like *Tyrannochromis nigriventer*, *Copadichromis virginalis*, and *Caprichromis liemi* that

265 have feeding motions in which kinesis is disproportionately concentrated toward the end of the

266 strike (i.e., high *kinesis skew*, and *motion patterns* with large positive PC 1 scores in fig. 3B).

267

268 ***Occupation of novel functional spaces***

269   Comparisons of hypervolumes identified whether individual radiations occupied unique

270 regions of multivariate functional spaces. For the *motion components*, we found that 62% of

271 Lake Tanganyika's and 49% of the Neotropics' functional space was unique to those radiations

272 at the exclusion of all others, with both results occurring in the 99th percentile of randomized

273 trials (fig. 3A; table S4). Cichlids occupying unique regions of the *kinematic components*

274 functional space in Tanganyika included several specialized planktivores with high upper jaw

275 protrusion in the genus *Cyprichromis* and elongate species with comparatively small gapes, like

276 *Chalinochromis brichardi* and *Julidochromis dickfeldi*. In the Neotropics, multiple species of

277 *Amatitlania* and a host of species in the tribe Geophagini (all with relatively small mouths, low

278 cranial rotation, and low hyoid depression) occurred in one unique region, and species capable of

279 extreme upper jaw protrusion, *Petenia splendida* and *Caquetaia myersi*, were found in another.

280 In contrast to Tanganyika and the Neotropics, only 6% of this space in Lake Malawi and 3% in

281 Lake Victoria was unique to those lakes, suggesting that most of their diversity is nested within

282 the other cichlid radiations (fig. 3A; table S4).

283   Across all species, the diversity of *motion patterns* was largely restricted to a distinct

284 concave or arched distribution (fig. 3B). This reflects a general constraint on motion diversity –

285 despite differences in the relative magnitude of movements (*motion components*), patterns of

286 feeding movements in cichlids are created by the same morphological features, moving in the

287 same direction, and mostly in the same sequence. One extreme of the *motion pattern* distribution

288 was characterized by an abrupt shift in the direction of cranial shape change within morphospace

289 toward the end of the motion, which manifested as an asymmetrical trajectory shape (left side of

290 fig. 3B). During feeding sequences, this was caused by late onset cranial rotation and hyoid

291 depression after full protrusion of the upper jaw was achieved, presumably for continued buccal

292 expansion posteriorly to prolong suction during prey acquisition. The other extreme contained

293 symmetrically shaped trajectories in which the rate of cranial shape change was slow initially but

294 fast toward the end of the strike, such that kinesis was disproportionately concentrated in later

295 motion stages (right side of fig. 3B), a pattern reminiscent of high *kinesis skew*. Comparisons of

296 hypervolumes for *motion pattern* revealed a mostly nested pattern in which Tanganyika (54%)

297   occupied the greatest volume of unique space (upper 99th percentile of permutations), with much

298   lower values for the Neotropics (26%), Malawi (14%), and Victoria (1%; table S4).

299

300   ***Rates of functional evolution***

301   Across all functional traits, there was a strong inverse and nonlinear relationship between

302   rates and crown ages of radiations (fig. S2; table S5). In each case, Lake Victoria had much

303   higher rates than other radiations, ranging anywhere from 42 to 95-fold faster diversification

304   compared to the radiation with the slowest rate. Similarly, the second youngest radiation, Lake

305   Malawi, consistently had the second highest rates of trait evolution. Pairwise comparisons of

306   rates between Lakes Victoria and Malawi were statistically significant at the α=0.05 level for

307   functional traits except for *hyoid depression* and *kinesis skew*. One caveat is that these analyses

308   assume a tree-like pattern of lineage diversification, and so we limit our interpretation primarily

309   to emphasize the vastly different time scales over which functional trait diversity has

310   accumulated in these radiations. In comparisons between the two older radiations, rates in Lake

311   Tanganyika were always higher than in the Neotropics, ranging from 1.1-fold to 4-fold

312   differences. However, unlike other pairwise comparisons among radiations, Tanganyika and the

313   Neotropics failed to show significant differences with each other for over half of the functional

314   traits considered. Significant differences in rate of evolution in these two radiations were found

315   for *premaxillary protrusion*, *kinesis skew*, *kinesis*, *motion components*, and *motion pattern*.

316

317   ***Modes of functional diversification***

318   Disparity through time (DTT) analyses provided information about temporal patterns of

319   diversification for two multivariate functional traits, *motion components* and *motion pattern*. In

320   Lake Tanganyika and the Neotropics, neither trait displayed DTT trends that were statistically

321   different from Brownian motion – the morphological disparity index (MDI), describing the

322   deviation of observed DTT trends from the null expectation, was not statistically significant for

323   either dataset (fig. 4A; see table S6 for results from all radiations). However, while DTT trends

324   for *motion components* largely stayed within the 95% range of simulated trait histories, those for

325   *motion pattern* were above the Brownian expectation in all radiations, in some cases for

326   prolonged durations, suggesting that trait variance was at times disproportionately concentrated

327   within subclades. Notably, none of the functional DTT trends fell below the lower 95% range for

328   Brownian motion, an indicator of early bursts of trait diversification during adaptive radiation

329   (fig. 4C).

330   Trait dispersion of extant species in each radiation around their most recent common

331   ancestor (MRCA) additionally captured patterns of trait space occupation across radiations at

332   different stages of development. Euclidean distances of *motion components* between species and

333   the MRCA were continuously distributed for all radiations except Lake Victoria (fig. 4B). In this

334   youngest lake, a handful of species with comparably low upper jaw protrusion formed a small

335   secondary peak that was more distantly situated from the Lake Victoria radiation MRCA

336   (observations in the upper left of the Lake Victoria distribution in fig. 3A). These species

337   consisted mostly of herbivorous cichlids from the genus *Neochromis* and omnivores in the genus

338   *Pundamilia*, possibly representing a (weakly) isolated adaptive peak related to trophic ecology

339   and jaw function. For *motion pattern*, Procrustes distances from radiation-specific MRCAs were

340   right-skewed, particularly in Lake Victoria and the Neotropics, seemingly reflecting the highly

341   constrained distribution of the trait more than distinct adaptive zones (figs. 3B & 4D).

342

343   *Cranial morphology and its relation to motion diversity*

344   Interspecific variance in head shape was highest in Neotropical cichlids, but only

345   marginally greater than in Lake Tanganyika (table S3). Still, the Neotropics boasted 2.3-times

346   more head shape diversity than Lake Malawi and 2.7-times more than Lake Victoria. Pairwise

347   comparisons of variances were statistically significant except between the two youngest

348   radiations, Malawi-Victoria, and the two oldest, Neotropics-Tanganyika (table S3). Interestingly,

349   the high head shape variance in the Neotropics did not directly translate to functional diversity,

350   as Lake Tanganyika still had greater (but similar) diversity in *motion components*, and

351   significantly higher variance in *kinesis*, *motion pattern, premaxillary protrusion*, and *maxillary*

352   *rotation* (fig. 5C-E).

353   Comparisons of hypervolumes for head shape revealed that 59% of cranial diversity in

354   the Neotropics and 57% in Lake Tanganyika was unique to those regions, both observations

355   occurring in the upper 99th percentile of randomized permutations (table S4). One of the things

356   that made the Neotropics stand out was expansion towards deep-headed taxa, like *Symphysodon*

357   *discus* and *Pterophyllum scalare*, but also several species in the genus *Amatitlania* that were not

358   as extreme but still outside of the space occupied by cichlids in other radiations (fig. 5A, lower

359   scores on PC 1). Some species from the African lake radiations occurred in a non-overlapping

360   region of morphospace with the Neotropics that contained many small-mouthed benthic biting

361   and picking specialists, like *Tropheus brichardi*, *Melanochromis wochepa*, and *Chalinochromis*

362   *popelini* (fig. 5A, lower scores on PC 2). In addition, Lake Tanganyika possessed a fair degree of

363   unique morphologies varying broadly in direction of mouth orientation (fig. 5B), from upturned

364   (e.g., *Haplotaxodon microlepis*) to downward deflecting profiles (e.g., *Xenotilapia ochrogenys*).

365   Morphological diversity within Lakes Malawi and Victoria was almost entirely contained within

366   the other regions, with only 5% and 3% unique morphospace occupation, respectively.

367   Rates of head shape evolution were again lowest in the older radiations (Neotropics and

368   Lake Tanganyika), faster in Lake Malawi and much faster in Lake Victoria (fig. S2; table S5).

369   All pairwise comparisons of rates were statistically significant (table S5). Like functional

370   analyses, disparity through time (DTT) trends for head shape were statistically indistinguishable

371   from a Brownian process (fig. S3; table S6). However, in the Neotropics the DTT trend dipped

372   just below the 95% range for Brownian simulations briefly from 44-40 Mya, and again for an

373   extended time from about 39 to 28 Mya (fig. S3). During these periods, head shape disparity was

374   concentrated among clades at a level beyond the null expectation, likely representing evolution

375   of clades towards different adaptive peaks.

376

377   **Discussion**

378   In this study, we provide the first quantitative comparison of functional diversity across

379   four major cichlid radiations, leveraging the largest-ever comparative kinematics dataset of

380   vertebrate organisms to contrast patterns of adaptive diversification across vastly different

381   temporal scales (many thousands of years to over 50 My) and spatial ranges (individual lakes

382   versus continental scale). We show that standing functional diversity in African cichlids is

383   strongly related to radiation age and displays a striking nested pattern in which trait spaces

384   occupied in Lakes Victoria and Malawi were almost fully contained within that of Lake

385   Tanganyika. Somewhat surprisingly, functional variance in the much older, continental

386   Neotropical radiation was lower than it was in Lake Tanganyika for many traits, making the high

387   diversity in the latter all the more impressive. This suggests that diversifying forces have

17

388   operated more effectively in Lake Tanganyika, and likely across the African Great Lakes, as

389   compared to the largely riverine cichlids of Central and South America. Indeed, numerous

390   cichlid lake radiations beyond those examined in this study experience elevated rates of

391   morphological evolution (Burress and Muñoz 2023).

392

393   ***Cichlid feeding systems and adaptive radiation***

394   Cichlids have long served as a model system for understanding adaptive radiation

395   (Stiassny and Meyer 1999; Seehausen 2006; Turner 2007), yet we recovered mixed evidence that

396   functional diversification of their feeding systems adheres to traditional expectations of this

397   process (Simpson 1953). A negative relationship was found between radiation age and rates of

398   kinematic and morphological evolution (fig. S2), suggesting that phenotypic diversification

399   proceeds fastest in early-stage radiations in a manner consistent with an early burst. Young

400   cichlid radiations in Lakes Victoria and Malawi support modest levels of trait diversity, but they

401   have acquired it at an incredibly fast pace. Although there may be some effect in our study of the

402   natural time-dependency of macroevolutionary rate estimates (Harmon et al. 2021), the

403   relationship between disparity and age of each radiation (fig. 2) strongly suggests a negative

404   correlation between age and rate of phenotypic diversification.

405   In addition to an early burst, an assumption of adaptive radiations remains that at some

406   stage of early diversification, trait variance will be distributed disproportionately among clades

407   versus within them (Simpson 1953; Harmon et al. 2003). Though cranial morphology showed

408   some hints of elevated divergence among lineages in the Neotropics (fig. S3), none of the

409   examined morphological or functional DTT trends were statistically different from Brownian

410   motion (table S6). Further, trait dispersion of extant species around their MRCA was mostly

411 continuous (fig. 4) with minimal evidence of clustering (i.e., discrete ecomorphs), a pattern

412 largely consistent across radiations. One exception was found for *motion components* in Lake

413 Victoria, which displayed a small secondary cluster of species with low values of jaw protrusion

414 (fig. 4B), possibly representing divergence toward an adaptive peak associated with a substrate

415 biting mode of feeding. That withstanding, comparably low trait variance in the two youngest

416 radiations (fig. 2) are not suggestive of rapid divergence *among* lineages occupying distinct

417 adaptive zones, where a significant portion of total potential diversity is achieved at initial stages

418 of adaptive expansion.

419   Our study suggests that the diversification of feeding systems in cichlid adaptive

420 radiations likely occurs by way of early burst, achieved not by adaptive divergence among

421 clades, but through extremely rapid within-clade dispersion in incipient radiations. Previous

422 research has predicted such patterns in cichlids as a possible outcome of transgressive

423 segregation during widespread introgression – a common theme of emerging African lake

424 radiations – paired with ecological opportunity in newly colonized habitats (Seehausen 2004;

425 Meier et al. 2017; Irisarri 2018; Salzburger 2018; Meier et al. 2019; Selz and Seehausen 2019).

426 Although we do not explicitly address the ecological dimensions across which functional

427 diversification occurs, previous work on Lake Malawi and Tanganyika cichlids suggests that

428 feeding diversity is distributed continuously along an axis of prey evasiveness (Martinez et al.

429 2018), matching observed patterns in this study of time-dependent trait dispersion around

430 radiation specific MRCAs (fig. 4). If the landscape of ecological opportunity was

431 discontinuously or sparsely distributed, for instance, it could pose challenges for a radiation

432 diversifying via transgressive segregation since open adaptive zones are no longer adjacent to

433   currently occupied zones, thereby reducing the probability that hybrid offspring happen upon a

434   more distantly situated adaptive peak.

435   Clear evidence for early bursts appears to be the exception and not the rule in

436   comparative trait data (Harmon et al. 2010). Previous analysis of trait diversification inclusive to

437   Lake Tanganyika cichlids showed support for an early burst in body shape evolution but failed to

438   find such evidence for jaw morphology (Ronco et al. 2021). Even this study, with rates among

439   radiations showing a strong slowing trend with age, did not satisfy the prediction of an early

440   burst by way of adaptive divergence among clades. Given that the latter is often used as a

441   diagnostic tool for identifying early bursts (Harmon et al. 2003), it raises questions about

442   potential limitations of our current models of adaptive radiation.

443

444   ***Are we watching the same film?***

445   Stephen Jay Gould famously contemplated what the diversity of life on earth might look

446   like if we had the ability to start over and replay the tape of life (Gould 1991). Would it be

447   unprecedented and unrecognizable, or would we see familiar patterns as selection inevitably

448   leads to diversification along predictable paths? Many others have since pondered this question

449   (e.g., Lobkovsky and Koonin 2012; Blount et al. 2018; Orgogozo 2015). In one sense, evolution

450   is constantly repeating its own version of this experiment at much smaller spatial and temporal

451   scales – independent radiations in related groups of organisms provide replication and insight

452   into evolutionary contingencies under conditions of varying similarity. A primary focus of this

453   study was to examine whether four large cichlid radiations, each resulting in hundreds of species

454   and celebrated levels of ecological and morphological variation, have generated similar patterns

455   of functional diversity. Has diversification of feeding functional morphology played out

456   following the same script in each radiation, or have they diversified along separate functional

457   axes? The answer appears to be that both are true.

458   Considering, for a moment, only the three African lake radiations examined in this study,

459   there is an argument to be made that both functional and morphological diversification have

460   progressed in a similar fashion in each of the lakes. The high-dimensional spaces filled by

461   *motion components*, *motion pattern*, and cranial shape data each show the younger radiations,

462   Malawi and Victoria, occupying subspaces of the older and more diverse Tanganyikan radiation,

463   with novelty only commonplace in the latter. This result is consistent with impressions of

464   widespread convergence on trophic morphotypes in Lakes Malawi and Tanganyika (Kocher et

465   al. 1993; Ronco et al. 2021). On the other hand, it is unclear if we were to fast-forward the Lake

466   Victoria tape to the current age of Lake Tanganyika (10-28 My, depending on the estimate),

467   whether we would find a carbon-copy of that lake or if selection would eventually lead the

468   Victorian radiation into unfamiliar functional and morphological spaces.

469   When we expand beyond the large African lake radiations to contrast their phenotypic

470   and functional diversity for the first time with the large Neotropical radiation, a different story

471   emerges. The two older radiations are more diverse than the others and each has invaded novel,

472   radiation-specific regions of functional and morphological space. Tanganyika boasts species with

473   unique combinations of *motion components*, including highly specialized planktivores

474   (*Cyprichomis*) and benthic foragers (e.g., *Pseudosimochromis curvifrons*, *Telamatochromis*

475   *vittatus*). In the Neotropics, some geophagine cichlids feed with a strongly sequenced kinematic

476   pattern, partitioned between distinct jaw protrusion and cranial rotation phases (asymmetrical

477   *motion patterns* toward the left of fig. 3B). Additionally, an innovation in select piscivorous

478   species from the tribe Heroini (e.g., *Petenia splendida* and *Caquetaia myersi*) results in extreme

479   levels of premaxillary protrusion (Waltzek and Wainwright 2003; Hulsey and García de León

480   2005) that places them in a unique region of *motion component* space (fig. 3A). Both Lake

481   Tanganyika and the Neotropics contain cichlids with functional profiles that do not occur

482   anywhere else, showing that radiations can eventually diverge from each other in key areas of

483   diversification. These observations amplify questions about the contrasting landscapes of

484   ecological opportunity experienced by lake versus continental radiations.

485

486   ***Morphology provides an imperfect index of functional diversity***

487   The idea that morphological variation can be used as a proxy for functional diversity is

488   commonly advanced, but the widespread presence of complex form-function relationships tests

489   this assumption (e.g., Wainwright et al. 2005; Young et al. 2007; 2010; Lautenschlager et al.

490   2020). Neotropical cichlids, when compared to the Lake Tanganyika radiation, illustrate that

491   high variance in cranial morphologies does not always result in greater functional diversity. The

492   primary axis of morphological variation in the Neotropics involved differences between elongate

493   and slender (e.g., *Crenicichla*) versus deep heads with steep cranial profiles (e.g., *Symphysodon*,

494   *Pterophyllum*, *Uaru*), which are adaptations typically found in species living in fast flowing

495   riverine environments and slow-moving water like lakes or floodplains, respectively (López-

496   Fernández et al. 2013). It is therefore likely that an important source of variance in head shapes

497   of Neotropical cichlids is due to selection on habitat-specific body shape, perhaps involving

498   adaptation of the locomotor system. Complex form-function relationships, particularly in

499   biomechanical systems with many cooperating components, can make for challenging

500   comparisons between morphologies and motions, and impact how these traits accumulate during

501   adaptive diversification (Alfaro et al. 2005). These findings suggest caution is warranted in

502   attributing observed morphological variation in fish feeding systems to functional diversity.

503

504   *Conclusions*

505   Cichlids have captivated the attention of biologists and aquarists alike with their

506   remarkable diversity, boasting seemingly endless combinations of body shapes, sizes, coloration

507   patterns, diets, and behaviors. Each radiation examined in this study has amassed an impressive

508   variety of morphological and functional diversity. Adaptive radiation of cichlids has produced

509   modest diversity of feeding kinematics in Lakes Victoria and Malawi, while Lake Tanganyika

510   has surpassed even the much older Neotropical radiation, suggesting that the forces driving

511   diversification in Tanganyika outstrip those in the Neotropics. However, these patterns of

512   diversity have been established on very different time scales. Rates of functional evolution range

513   from 40-95 times faster in Lake Victoria than in the Neotropics, supporting the notion that the

514   African Great Lake radiations have involved rapid evolutionary change. These observations

515   suggest that while similarities exist, adaptive radiation of cichlid feeding kinematics has not

516   always followed a common profile. Rather, evolutionary contingencies linked to time and

517   biogeography explain varied patterns of morphological and functional diversification across this

518   iconic group of fishes.

519

524   American Dissertation Fellowship from the American Association of University Women and a

525   fellowship from the Achievement Rewards for College Scientists Foundation. ASRH was

526   supported by the National Science Foundation with a Graduate Research Fellowship, Grant No.

527   1650042.

528

529   **Statement of Authorship**

530   CMM and PCW conceived of the project. MDM and SRB recorded most of the videos of cichlid

531   feeding events, and CMM contributed videos for the remaining species. All authors digitized

532   landmark data on video frames. KAC ran statistical analyses. CMM and PCW wrote the paper

533   with edits from all authors.

534

535   **Figure Captions**

536   **Figure 1.** Functional traits examined across 300 species of cichlid in this study. **A**) Principal

537   component axes, PC 1 and PC 2, displaying shape change for a single trajectory of 10 cranial

538   shapes during a suction feeding motion. **B**) Subsets of two or three landmarks were used to

539   measure maximum excursions of six commonly measured *motion components* of suction feeding

540   in percomorph fishes. **C**) Changes in the timing or extent of movements represent differences in

541   *motion pattern* that are manifested as variation in trajectory shapes. Trajectories varied in

542   spacing of cranial shape changes and the relative symmetry of trajectory paths. **D**) A series of

543   trajectory-derived traits related to mobility, included cranial *kinesis* (total trajectory length),

544   *kinesis coefficient* (not pictured, total output kinesis divided by input movement from cranial

545   rotation), and *kinesis skew* (kinesis over the last five motion shapes divided by total kinesis). **E**)

546   PCs 1 and 2 from 1,110 trajectories of suction feeding motions, with deformation grids

547   displaying shape change. All plots are shown in two dimensions for visualization, but data

548   analysis was in the full dimensionality of the shape data unless otherwise noted.

549

550   **Figure 2.** Functional trait variances in cichlid adaptive radiations plotted against crown age. Six

551   individual kinematic traits are shown on top, with an arrow pointing to the multivariate *motion*

552   *components* containing all of them. *Motion pattern* (i.e., the shape of a kinematic trajectory) is

553   shown in the middle with an arrow pointing to composite *kinesis-based* traits measured from

554   trajectories. Letters next to plot points denote significant P-values from pairwise comparisons.

555   Radiations sharing a letter do not have statistically different variances.

556

557   **Figure 3.** Primary dimensions of variation, PCs 1 and 2, from separate principal component

558   analyses for species-averaged multivariate functional traits. **A**) *Motion components*, a dataset

559   comprising measurements of maximum excursions for six key kinematic features are plotted by

560   cichlid radiation. Cichlid heads at maximum gape are shown across the plot, and trait loadings

561   are shown on the right. **B**) Variation in *motion patterns* by radiation, with two-dimensional

562   representations of the shapes of kinematic trajectories provided at select locations of the plot (red

563   diamonds). Low values on PC 1 are motions with an abrupt shift in the manner of cranial

564   movements and large values are motions in which kinesis is disproportionately concentrated

565   toward the end of the strike. For both multivariate traits, Lake Tanganyika and the Neotropics

566   display unique occupation of this space, while Lakes Malawi and Victoria are almost entirely

567   nested within them. Estimated values of most recent common ancestors (MRCA) are shown as

568   large dots with white borders.

569

Figure 4. Disparity through time (DTT) plots in the two oldest cichlid radiations, Lake Tanganyika and the Neotropics, for **A)** *motion components* and **C)** *motion pattern*. Also shown are distributions of **B)** Euclidean distances *of motion components* and **D)** Procrustes distances of *motion pattern* between extant species and their radiation-specific most recent common ancestor (MRCA).

Figure 5. Species-averaged interspecific head shape diversity across cichlid radiations. **A)** Major axes of variation, PCs 1 & 2, show the wide diversity of head shapes in Neotropical cichlids, most notably in head depth (left of plot). Small-mouthed taxa in African lakes, often benthic biting feeders, are concentrated toward the bottom of the plot. **B**) PCs 3 and 4 display axes on which Lake Tanganyika contains high morphological diversity, including variation in orientation of jaws. **C-E**) variance in head shape is shown in relation to select kinematic traits, displaying relationships between form and function. High morphological diversity in the Neotropics does not translate to commensurate kinematic diversity. Most recent common ancestors (MRCA) are shown as large dots with white borders.

Literature Cited

Adams, D. C., and M. M. Cerney. 2007. Quantifying biomechanical motion using Procrustes motion analysis. Journal of Biomechanics. 40:437–44.

Adams, D. C., and M. L. Collyer. 2009. A general framework for the analysis of phenotypic trajectories in evolutionary studies. Evolution 63:1143–54.

591   Adams, D., M. Collyer, A. Kaliontzopoulou, and E. Baken. 2021. "Geomorph: Software for

592   geometric morphometric analyses. R package version 4.0." https://cran.r-

593   project.org/package=geomorph.

594   Alfaro, M. E., D. I. Bolnick, and P. C. Wainwright. 2005. Evolutionary consequences of many-

595   to-one mapping of jaw morphology to mechanics in labrid fishes. American Naturalist

596   165:E140–E154.

597   Arbour, J. H., and H. López-Fernández. 2014. Adaptive landscape and functional diversity of

598   Neotropical cichlids: implications for the ecology and evolution of Cichlinae (Cichlidae;

599   Cichliformes). Journal of Evolutionary Biology 27:2431–2442.

600   Blonder, B., C. Lamanna, C. Violle, and B. J. Enquist. 2014. The n-dimensional hypervolume.

601   Global Ecology and Biogeography 23:595–609.

602   Blonder, B., C. B. Morrow, B. Maitner, D. J. Harris, C. Lamanna, C. Violle, B. J. Enquist, and

603   A. J. Kerkhoff. 2018. New approaches for delineating n-dimensional hypervolumes.

604   Methods in Ecology and Evolution 9:305–319.

605   Blount, Z. D., R. E. Lenski, and J. B. Losos. 2018. Contingency and determinism in evolution:

606   Replaying life's tape. Science 362:aam5979.

607   Burress, E. D., and M. M. Muñoz. 2023. Phenotypic rate and state are decoupled in response to

608   river-to-lake transitions in cichlid fishes. Evolution qpad143.

609   Burress, E. D., L. Piálek, J. R. Casciotta, A. Almirón, M. Tan, J. W. Armbruster, and O. Říčan.

610   2017. Island- and lake-like parallel adaptive radiations replicated in rivers. Proceedings

611   of the Royal Society B 285:20171762.

612 Camp, A. L., A. M. Olsen, L. P. Hernandez, and E. L. Brainerd. 2020. Fishes can use axial

613   muscles as anchors or motors for powerful suction feeding. Journal of Experimental

614   Biology 223:jeb225649.

615 Collyer, M. L., and D. C. Adams. 2013. Phenotypic trajectory analysis: comparison of shape

616   change patterns in evolution and ecology. Hystrix 24:75–83.

617 Collyer, M. L., and D. C. Adams. 2018. "RRPP: An R package for fitting linear models to high-

618   dimensional data using residual randomization."

619   https://besjournals.onlinelibrary.wiley.com/doi/10.1111/2041-210X.13029.

620 Collyer, M. L., and D. C. Adams. 2019. "RRPP: Linear Model Evaluation with Randomized

621   Residuals in a Permutation Procedure. R package version 1.0.0." https://CRAN.R-

622   project.org/package=RRPP.

623 Cooper, W. J., K. Parsons, A. McIntyre, B. Kern, A. McGee-Moore, and R. C. Albertson. 2010.

624   Bentho-pelagic divergence of cichlid feeding architecture was prodigious and consistent

625   during multiple adaptive radiations within African lift lakes. PLoS ONE 5:e9551.

626 Corn, K. A., S. T. Friedman, E. D. Burress, C. M. Martinez, O. Larouche, S. A. Price, and P. C.

627   Wainwright. 2022. The Rise of Biting During the Cenozoic Fueled Reef Fish Body

628   Shape Diversification. Proceedings of the National Academy of Sciences

629   119:e2119828119.

630 Delvaux, D. 1995. Age of Lake Malawi (Nyasa) and water level fluctuations. Musée Royal

631   Afrique Centrale, Tervuren (Belgique), Department de Geologie et Mineralogies, Rapport

632   Annuel 1995-1996:99-108.

633 Fryer, G., and T. D. Iles. 1972. The cichlid fishes of the Great Lakes of Africa. Oliver and Boyd,

634   Edinburgh.

635   Gillespie, R. G. 2013. Adaptive radiation: convergence and non-equilibrium. Current Biology

636   2:R71-R74

637   Gillespie, R. 2004. Community assembly through adaptive radiation in Hawaiian spiders.

638   Science 303:356-359

639   Gillespie, R. G., G. M. Bennett, L. De Meester, J. L. Feder, R. C. Fleischer, L. J. Harmon, A. P.

640   Hendry, M. L. Knope, J. Mallet, C. Martin, and C. E. Parent. 2020. Comparing adaptive

641   radiations across space, time, and taxa. Journal of Heredity, 111:1-20.

642   Gould, S. J. 1991. Wonderful life – the Burgess shale and the nature of history. WW. Norton &

643   Company, New York.

644   Greenwood, P. H. 1980. Towards a phyletic classification of the 'genus' *Haplochromis* (Pisces,

645   Cichlidae) and related taxa. Part 2; the species from Lakes Victoria, Nabugabo, Edward,

646   George and Kivu. Bulletin of the British Museum (Natural History) Zoology. 39:1-101.

647   Harmon, L. J., J. B. Losos, T. J. Davies, R. G. Gillespie, J. L. Gittleman, W. B. Jennings, K. H.

648   Kozak, M. A. McPeek, F. Moreno-Roark, T. J. Near, A. Purvis, R. E. Ricklefs, D.

649   Schluter, J. A. Schulte II, O. Seehausen, B. L. Sidlauskas, O. Torres-Carvajal, J. T.

650   Weir, and O. Mooers, A. 2010. Early bursts of body size and shape evolution are rare in

651   comparative data. Evolution. 64:2385-2396.

652   Harmon, L. J., M. W. Pennell, L. F. Henao-Diaz, J. Rolland, B. N. Sipley, and J. C. Uyeda. 2021.

653   Causes and consequences of apparent timescaling across all estimated evolutionary

654   rates. Annual Review of Ecology, Evolution, and Systematics 52:587-609.

655   Harmon, L. J., J. A. Schulte, A. Larson, and J. B. Losos. 2003. Tempo and mode of evolutionary

656   radiation in iguanian lizards. Science 301:961-964.

657   Harmon, L. J., J. T. Weir, C. D. Brock, R. E. Glor, and W. Challenger. 2008. GEIGER:

658   Investigating evolutionary radiations. Bioinformatics 24:129–131.

659   Higham, T. E., C. D. Hulsey, O. Říčan, and A. M. Carroll. 2007. Feeding with speed: prey

660   capture evolution in cichlids. Journal of Evolutionary Biology 20:70-78

661   Hulsey, C. D., and F. J. García De León. 2005. Cichlid jaw mechanics: linking morphology to

662   feeding specialization. Functional Ecology 19:487-494.

663   Hulsey, C. D., F. J. García De León, and R. Rodiles-Hernandez. 2006. Micro- and

664   macroevolutionary decoupling of cichlid jaws: A test of Liem's key innovation

665   hypothesis. Evolution 60:2096-2109.

666   Huttegger, S. M., and P. Mitteroecker. 2011. Invariance and meaningfulness in phenotype

667   spaces. Evolutionary Biology 38:335-351.

668   Irisarri, I., P. Singh, S. Koblmüller, J. Torres-Dowdall, F. Henning, P. Franchini, C. Fischer, A.

669   R. Lemmon, E. M. Lemmon, G. G. Thallinger, C. Sturmbauer, and A. Meyer. 2018.

670   Phylogenomics uncovers early hybridization and adaptive loci shaping the radiation of

671   Lake Tanganyika cichlid fishes. Nature Communications 9:3159.

672   Joyce, D. A., D. H. Lunt, M. J. Genner, G. F. Turner, R. Bills, and O. Seehausen. 2011. Repeated

673   colonization and hybridization in Lake Malawi cichlids. Current Biology 21:R108–R109

674   Kocher, T. D., J. A. Conroy, K. R. McKaye, and J. R. Stauffer. 1993. Similar morphologies of

675   cichlid fish in Lakes Tanganyika and Malawi are due to convergence. Molecular

676   Phylogenetics and Evolution 2:158–165.

677   Lautenschlager, S., B. Figueirido, D. D. Cashmore, E.-M. Bendel, and T. L. Stubbs. 2020.

678   Morphological convergence obscures functional diversity in sabre-toothed carnivores.

679   Proceedings of the Royal Society B 287:20201818.

680 Lobkovsky, A. E., and E. V. Koonin. 2012. Replaying the tape of life: quantification of the

681   predictability of evolution. Frontiers in Genetics 3:246.

682 López-Fernández, H., J. H. Abrbour, K. O. Winemiller, and R. L. Honeycutt. 2013. Testing for

683   ancient adaptive radiation in Neotropical cichlid fishes. Evolution 67:1321-1337.

684 Losos, J. B., T. R. Jackman, A. Larson, K. D. Queiroz, and L. Rodríguez-Schettino. 1998.

685   Contingency and determinism in replicated adaptive radiations of island lizards. Science

686   279:2115-2118.

687 Martinez, C. M., and P. C. Wainwright. 2019. Extending the geometric approach for studying

688   biomechanical motions. Integrative and Comparative Biology 59:684-695.

689 Martinez, C. M., M. D. McGee, S. R. Borstein, and P. C. Wainwright. 2018. Feeding ecology

690   underlies the evolution of cichlid jaw mobility. Evolution 72:1645-1655.

691 Martinez, C. M., A. Tovar, and P. C. Wainwright. 2022. A novel intramandibular joint facilitates

692   feeding versatility in the sixbar distichodus. Journal of Experimental Biology

693   225:jeb243621.

694 Matschiner, M. 2018 Gondwanan vicariance or trans-Atlantic dispersal of cichlid fishes: a

695   review of the molecular evidence. Hydrobiologia 832:9-37.

696 Matschiner, M., A. Böhne, F. Ronco, and W. Salzburger. 2020 The genomic timeline of cichlid

697   fish diversification across continents. Nature Communications 11:5895.

698 McGee, M. D., S. R. Borstein, J. I. Meier, D. A. Marques, S. Mwaiko, A. Taabu, M. A. Kishe, B.

699   O'Meara, R. Bruggmann, L. Excoffier, and O. Seehausen. 2020. The ecological and

700   genomic basis of explosive adaptive radiation. Nature 586:75-79.

701 McGee, M. D., B. C. Faircloth, S. R. Borstein, J. Zheng, C. D. Hulsey, P. C. Wainwright, and M.

702   E. Alfaro. 2016. Replicated divergence in cichlid radiations mirrors a major vertebrate

703   innovation. Proceedings of the Royal Society B 283:20151413.

704 Meier, J. I., D. A. Marques, S. Mwaiko, C. E. Wagner, L. Excoffier, and O. Seehausen. 2017.

705   Ancient hybridization fuels rapid cichlid fish adaptive radiations. Nature

706   Communications 8:14363.

707 Meier, J. I., R. B. Stelkens, D. A. Joyce, S. Mwaiko, N. Phiri, U. K. Schliewen, O. M. Selz, C. E.

708   Wagner, C. Katongo, and O. Seehausen. 2019. The coincidence of ecological

709   opportunity with hybridization explains rapid adaptative radiation in Lake Mweru

710   cichlid fishes. Nature Communications 10:5391.

711 Olsen, A., and M. Westneat. 2015. "StereoMorph: an R package for the collection of 3D

712   landmarks and curves using a stereo camera set-up." Methods in Ecology and Evolution

713   6:351-356.

714 Orgogozo, V. 2015. Replaying the tape of life in the twenty-first century. Interface Focus

715   5:20150057.

716 Patton, A. H., E. J. Richards, K. J. Gould, L. K. Buie, and C. H. Martin. 2022. Hybridization

717   alters the shape of the genotypic fitness landscape, increasing access to novel fitness

718   peaks during adaptive radiation. Elife 11:e72905.

719 Pennell, M., J. Eastman, G. Slater, J. Brown, J. Uyeda, R. Fitzjohn, M. Alfaro, and L. Harmon.

720   2014. "geiger v2.0: an expanded suite of methods for fitting macroevolutionary models

721   to phylogenetic trees." Bioinformatics 30:2216-2218.

722 R Core Team. 2021. R: A language and environment for statistical computing. R Foundation for

723   Statistical Computing, Vienna, Austria. URL https://www.R-project.org/.

724   Rohlf, F. J. 2015. The tps series of software. Histrix 26:9–12.

725   Ronco, F., M. Matschiner, A. Böhne, A. Boila, H. H. Büscher, A. El Taher, A. Indermaur, M.

726   Malinsky, V. Ricci, A. Kahman, S. Jentoft, and W. Salzburger. 2021. Drivers and

727   dynamics of massive adaptive radiation in cichlid fishes. Nature 589:76-81.

728   Salzburger, W. 2018. Understanding explosive diversification through cichlid fish genomics.

729   Nature Reviews Genetics 19:705-717.

730   Scherz, M. D., P. K. Masonick, A. Meyer, and C. D. Hulsey. 2022. Between a rock and a hard

731   polytomy: phylogenomics of the rock-dwelling mbuna cichlids of Lake Malaŵi.

732   Systematic Biology 71:741-757.

733   Schluter, D. 1996. Adaptive radiation along genetic lines of least resistance. Evolution 50:1766-

734   1774.

735   Seehausen, O. 1996. Lake Victoria rock cichlids, taxonomy, ecology and distribution. Verduijn

736   Cichlids, Zevenhuizen, Netherlands.

737   Seehausen, O. 2004. Hybridization and adaptive radiation. Trends in Ecology and Evolution

738   19:198-207.

739   Seehausen, O. 2006. African cichlid fishes, a model system in adaptive radiation research.

740   Proceedings of the Royal Society B 273:1987-1998.

741   Seehausen, O., E. Lippitsch, N. Bouton, H. Zwennes. 1998. Mbipi, the rock-dwelling cichlids of

742   Lake Victoria: description of three new genera and fifteen new species (Teleostei).

743   Ichthyological Exploration of Freshwaters 9:129-228.

744   Selz, O. M., and O. Seehausen. 2019. Interspecific hybridization can generate functional novelty

745   in cichlid fish. Proceedings of the Royal Society B 286:20191621.

746   Simpson, G. G. 1953. The major features of Evolution. Columbia University Press, New York.

747   Sparks, J. S. 2004. Molecular phylogeny and biogeography of the Malagasy and South Asian

748   cichlids (Teleostei: Perciformes: Cichlidae). Molecular Phylogenetics and Evolution.

749   30:599–614.

750   Sparks, J. S., and W. L. Smith. 2004. Phylogeny and biogeography of cichlid fishes (Teleostei:

751   Perciformes: Cichlidae). Cladistics 20:501–517.

752   Stager, J. C., and T. C. Johnson. 2008. The late Pleistocene desiccation of Lake Victoria and the

753   origin of its endemic biota. Hydrobiologia 596:5-16.

754   Stiassny, M. L. J., and A. Meyer. (1999). Cichlids of the rift lakes, Scientific American 280:64-

755   69.

756   Tokita, M., W. Yano, H. F. James, and A. Abzhanov. 2016. Cranial shape evolution inadaptive

757   radiations of birds: comparative morphometrics of Darwin's finches and Hawaiian

758   honeycreepers. Philosophical Transactions of the Royal Society B 372:20150481.

759   Turner, G. F. 2007. Adaptive radiation of cichlid fish. Current Biology 17:R827-R831.

760   Wainwright, P. C., M. E. Alfaro, D. I. Bolnick, and C. D. Hulsey. 2005. Many-to-one mapping

761   of form to function: a general principle in organismal design? Integrative and

762   Comparative Biology 45:256–262.

763   Waltzek, T. B., and P. C. Wainwright. 2003. Functional morphology of extreme jaw protrusion

764   in Neotropical cichlids. Journal of Morphology 257:96-106.

765   Westneat, M. W. 1994. Transmission of force and velocity in the feeding mechanisms of labrid

766   fishes (Teleostei, Perciformes). Zoomorphology 114:103-118.

767   Westneat, M. W. 2004. Evolution of Levers and Linkages in the Feeding Mechanisms of Fishes.

768   Integrative and Comparative Biology 44:378-389.

769   Young, K. A., J. Snoeks, and O. Seehausen. 2009. Morphological Diversity and the Roles of

770   Contingency, Chance and Determinism in African Cichlid Radiations. PLoS ONE

771   4:e4740.

772   Young, R. L., T. S. Haselkorn, and A. V. Badyaev. 2007. Functional equivalence of

773   morphologies enables morphological and ecological diversity. Evolution 61:2480–2492.

774   Young, R. L., M. J. Sweeney, and A. V. Badyaev. 2010. Morphological diversity and ecological

775   similarity: versatility of muscular and skeletal morphologies enables ecological

776   convergence in shrews. Functional Ecology 24:556-565.
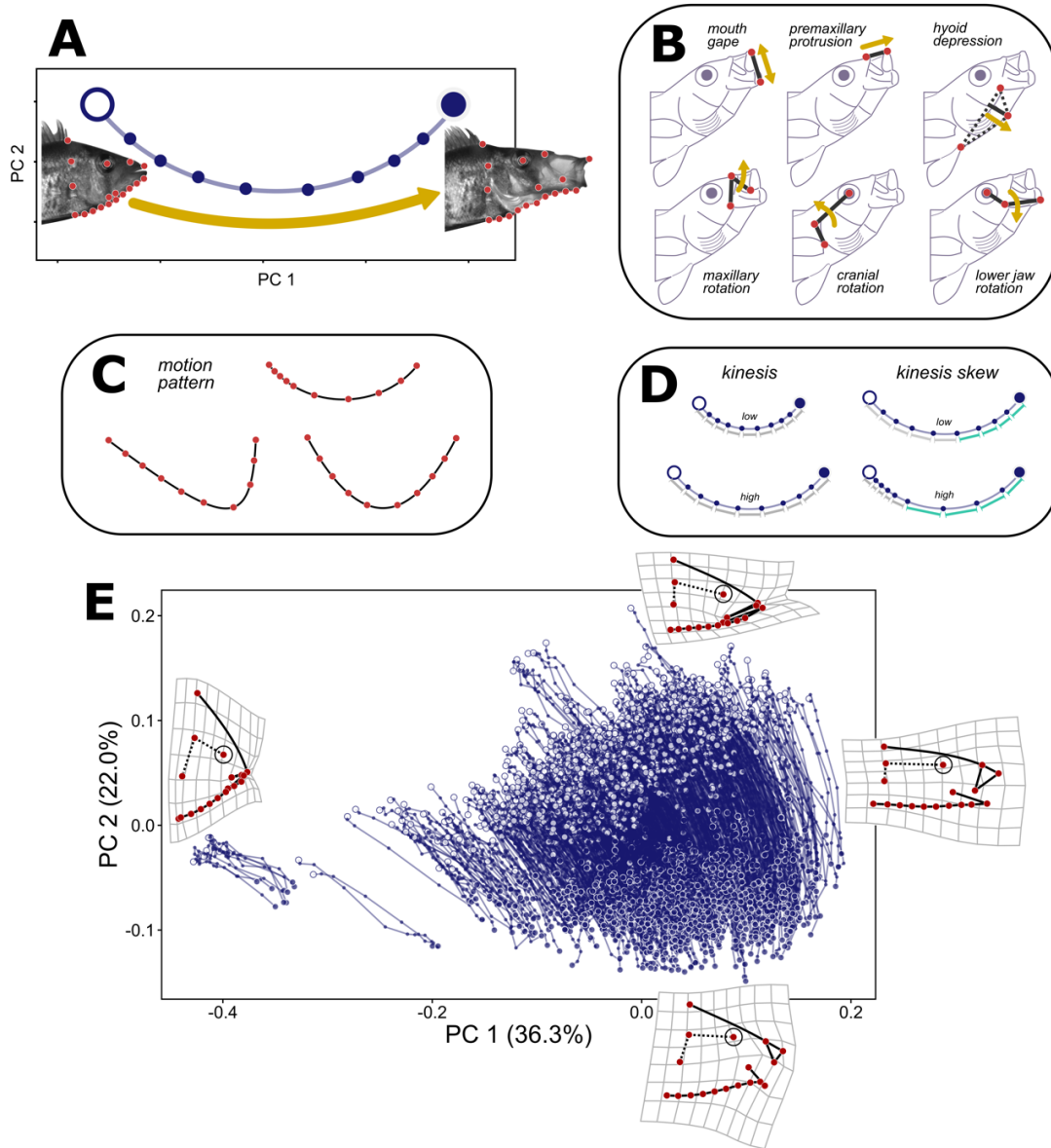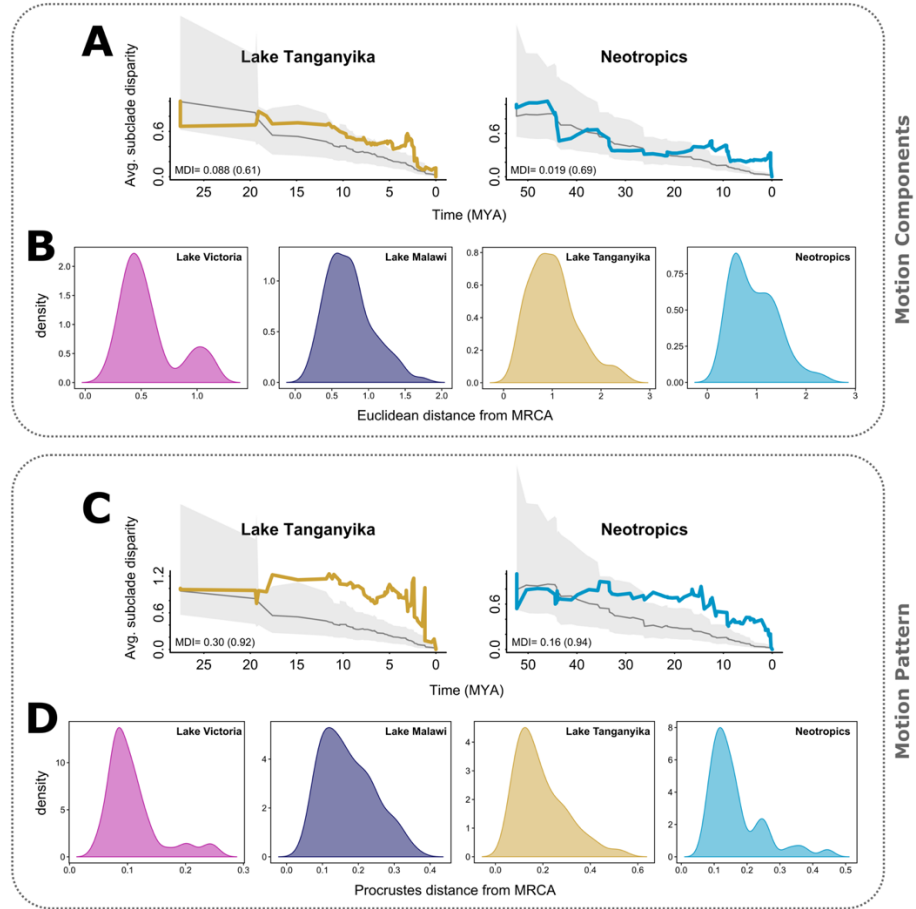
Figure 1. Functional traits examined across 300 species of cichlid in this study. A) Principal component axes, PC 1 and PC 2, displaying shape change for a single trajectory of 10 cranial shapes during a suction feeding motion. B) Subsets of two or three landmarks were used to measure maximum excursions of six commonly measured motion components of suction feeding in percomorph fishes. C) Changes in the timing or extent of movements represent differences in motion pattern that are manifested as variation in trajectory shapes. Trajectories varied in spacing of cranial shape changes and the relative symmetry of trajectory paths. D) A series of trajectory-derived traits related to mobility, included cranial kinesis (total trajectory length), kinesis coefficient (not pictured, total output kinesis divided by input movement from cranial rotation), and kinesis skew (kinesis for the last five motion shapes divided by total kinesis). E) PCs 1 and 2 from 1,110 trajectories of suction feeding motions, with deformation grids displaying shape change. All plots are shown in two dimensions for visualization, but data analysis was in the full dimensionality of the shape data unless otherwise noted.
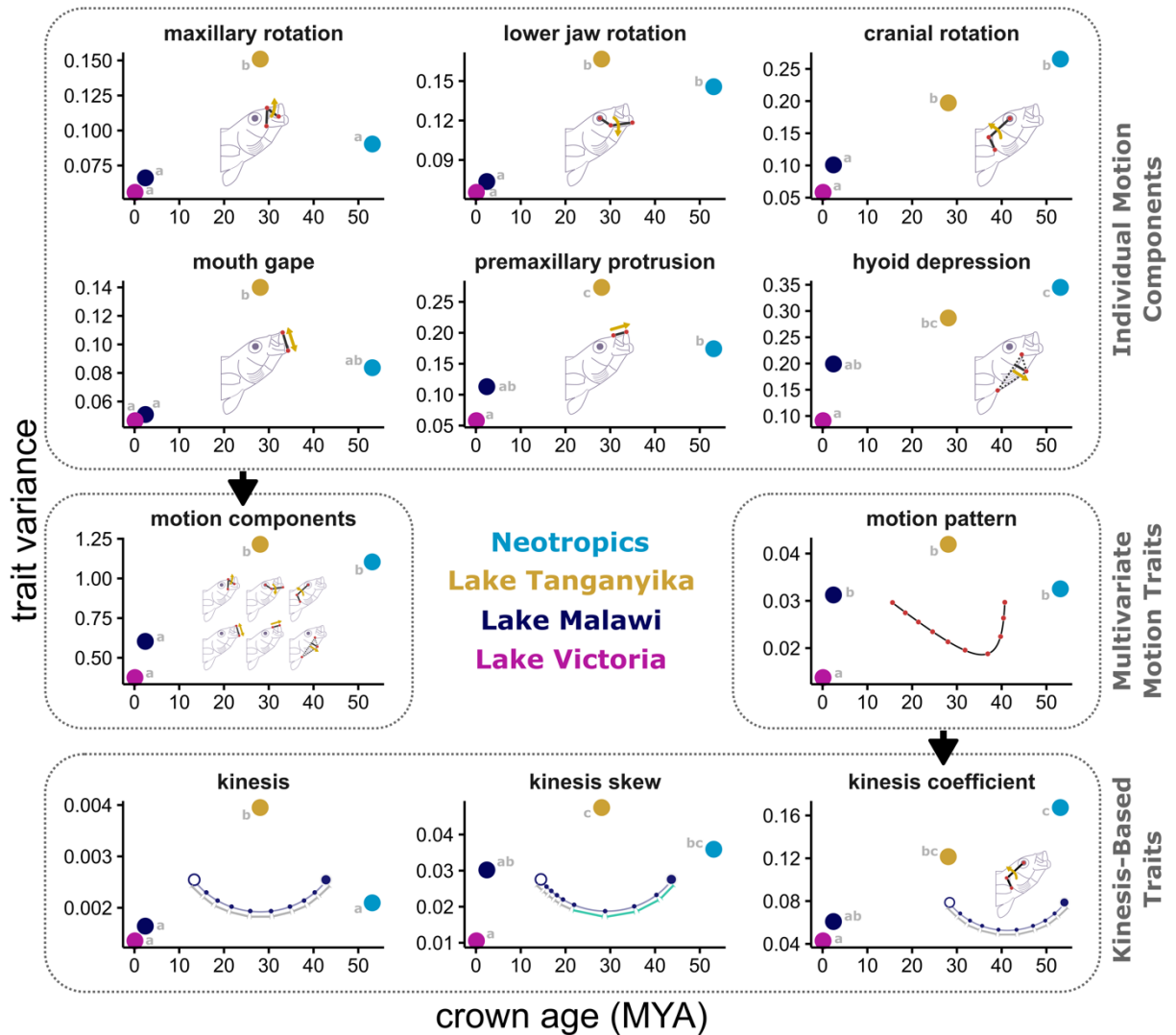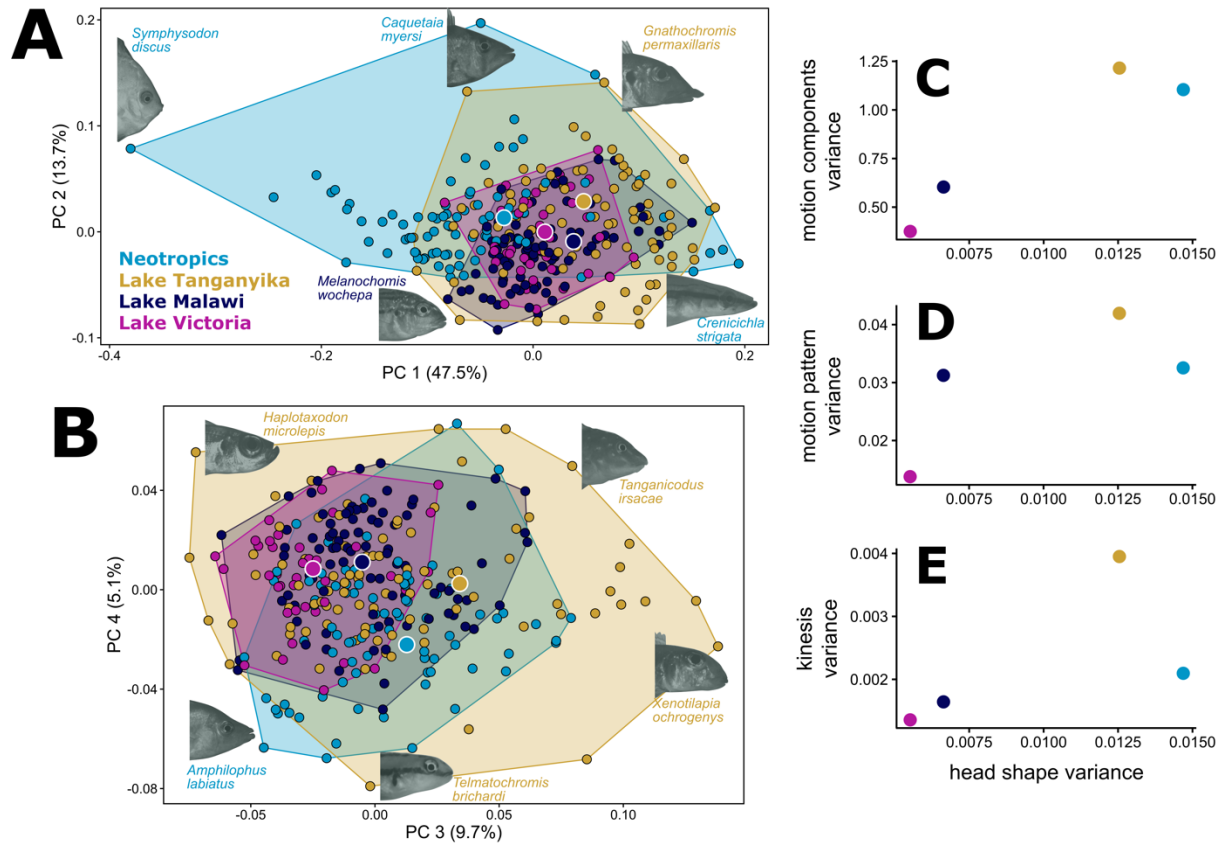
Figure 2. Functional trait variances in cichlid adaptive radiations plotted against crown age. Six individual kinematic traits are shown on top, with an arrow pointing to the multivariate motion components containing all of them. Motion pattern (i.e., the shape of a kinematic trajectory) is shown in the middle with an arrow pointing to composite kinesis-based traits measured from trajectories. Letters next to plot points denote significant P-values from pairwise comparisons. Radiations sharing a letter do not have statistically different variances.
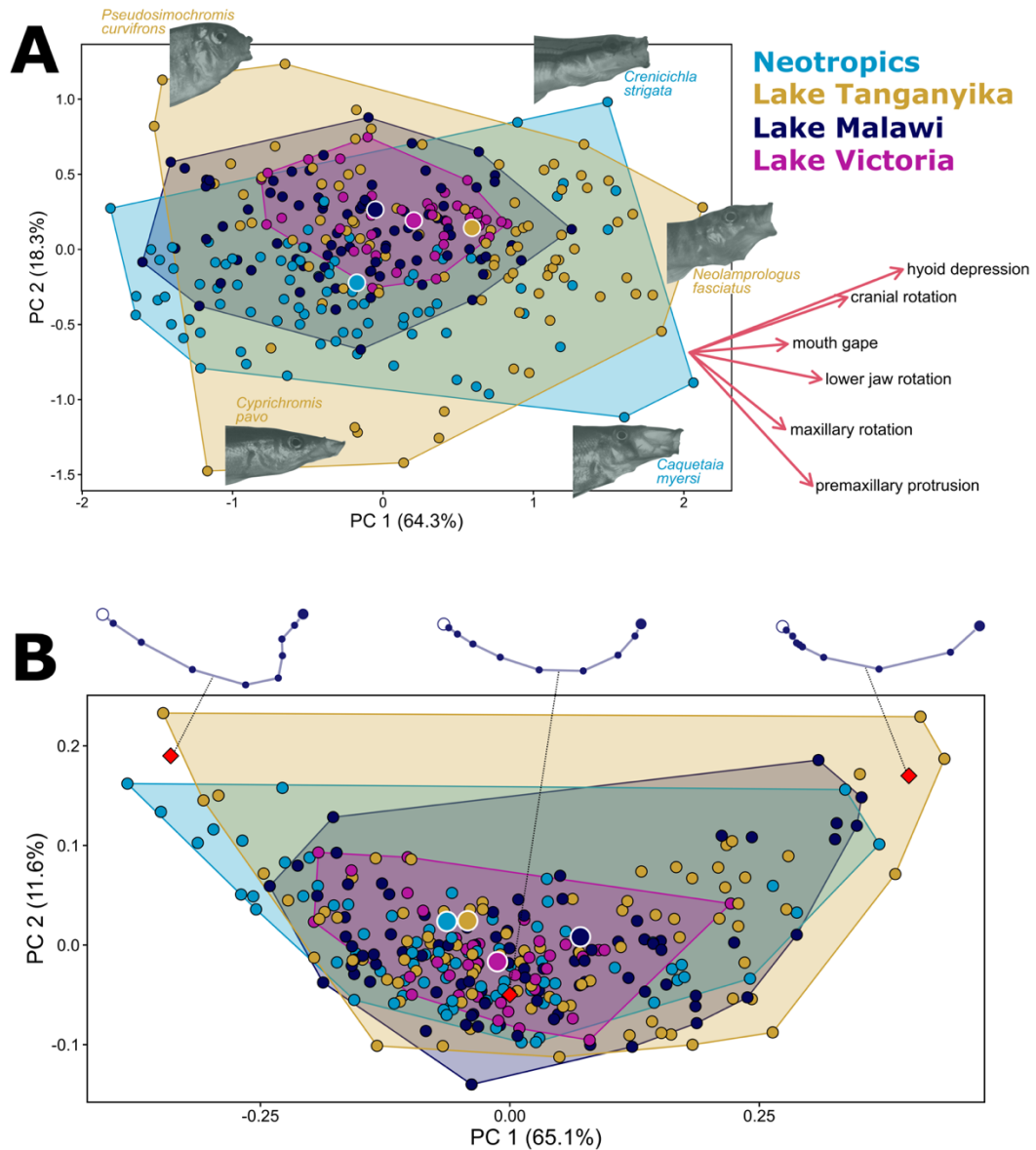
Figure 3. Primary dimensions of variation, PCs 1 and 2, from separate principal component analyses for species-averaged multivariate functional traits. A) Motion components, a dataset comprising measurements of maximum excursions for six key kinematic features are plotted by cichlid radiation. Cichlid heads at maximum gape are shown across the plot, and trait loadings are shown on the right. B) Variation in motion patterns by radiation, with two-dimensional representations of the shapes of kinematic trajectories provided at select locations of the plot (red diamonds). Low values on PC 1 are motions with an abrupt shift in the manner of cranial movements and large values are motions in which kinesis is disproportionately concentrated toward the end of the strike. For both multivariate traits, Lake Tanganyika and the Neotropics display unique occupation of this space, while Lakes Malawi and Victoria are almost entirely nested within them. Estimated values of most recent common ancestors (MRCA) are shown as large dots with white borders.

Figure 4. Disparity through time (DTT) plots in the two oldest cichlid radiations, Lake Tanganyika and the Neotropics, for A) motion components and C) motion pattern. Also shown are distributions of B) Euclidean distances of motion components and D) Procrustes distances of motion pattern between extant species and their radiation-specific most recent common ancestor (MRCA).

Figure 5. Species-averaged interspecific head shape diversity across cichlid radiations. A) Major axes of variation, PCs 1 & 2, show the wide diversity of head shapes in Neotropical cichlids, most notably in head depth (left of plot). Small-mouthed taxa in African lakes, often benthic biting feeders, are concentrated toward the bottom of the plot. B) PCs 3 and 4 display axes on which Lake Tanganyika contains high morphological diversity, including variation in orientation of jaws. C-E) variance in head shape is shown in relation to select kinematic traits, displaying relationships between form and function. High morphological diversity in the Neotropics does not translate to commensurate kinematic diversity. Most recent common ancestors (MRCA) are shown as large dots with white borders.